European Spine Journal
https://doi.org/10.1007/s00586-022-07303-x

ORIGINAL ARTICLE

Venous injection of a triphasic calcium-based implant in a sheep model of pulmonary embolism demonstrates minimal acute systemic effects

Caroline Constant[1] · John D. Stroncek[2] · Stephan Zeiter[1] · Daniel Arens[1] · Dirk Nehrbass[1] · Dominic Gehweiler[1] · Ursula Menzel[1] · Lorin M. Benneker[3] · Ronald S. Hill[2] · Christoph E. Albers[4]

Received: 17 March 2022 / Revised: 17 March 2022 / Accepted: 24 June 2022

Abstract

Purpose Implant leakage is the most common complication of vertebral augmentation. Alternative injectable materials must demonstrate intravascular safety comparable to or better than polymethyl methacrylate (PMMA). This study assessed the systemic effects of a triphasic calcium-based implant or PMMA injected directly into the femoral vein in a large animal model designed to mimic severe intravascular implant leakage.

Methods Six skeletally mature female sheep were randomly assigned ($n=3$) to either the PMMA or the triphasic implant (AGN1, composition: calcium sulfate, β-tricalcium phosphate, brushite) treatment group. Femoral veins of each sheep were directly injected with 0.5 mL of implant material to mimic leakage volumes reported during PMMA vertebroplasty. To compare acute systemic effects of the materials, cardiovascular parameters, laboratory coagulation markers, and calcium and sulfate serum levels were monitored for 60 min after implant injection. Thrombotic and embolic events were evaluated by radiologic imaging, necropsy, and histopathology.

Results Heart rate, systemic arterial blood pressure, arterial oxygenation, arterial carbon dioxide content, and coagulation markers remained within physiological range after either AGN1 or PMMA injection. No blood flow interruption in the larger pulmonary vessels was observed in either group. Lung histopathology revealed that the severity of thrombotic changes after AGN1 injection was minimal to slight, while changes after PMMA injection were minimal to massive.

Conclusion Acute systemic effects of intravascular AGN1 appeared to be comparable to or less than that of intravascular PMMA. Furthermore, in this preliminary study, the severity and incidence of pulmonary histological changes were lower for AGN1 compared to PMMA.

Keywords Triphasic calcium implant · PMMA · Vertebral augmentation · Vertebroplasty · Kyphoplasty · Pulmonary embolism

Introduction

Painful compression fractures of vertebral bodies occur in spines weakened by osteoporosis, hemangioma, or metastases. These fractures can cause persistent pain, impairing patient mobility, and reducing quality of life [1]. In selected patients, minimally invasive vertebral augmentation provides lasting pain relief, increases patient quality of life and decreases health deterioration, hospitalization time, costs, and mortality risk compared to conservative therapy [2–6].

Vertebral augmentation is routinely performed with polymethyl methacrylate (PMMA) bone cement. PMMA has significant limitations including high stiffness that can alter spine biomechanics, increasing the likelihood of additional

✉ John D. Stroncek
jstroncek@agnovos.com

1 AO Research Institute Davos, Davos, Switzerland

2 AgNovos Healthcare, 7301 Calhoun Place Suite 100, Rockville, MD 20855, USA

3 Spine Surgery, Sonnenhofspital, University of Bern, Bern, Switzerland

4 Inselspital, University Hospital Bern, Bern, Switzerland

Published online: 17 August 2022

surgical interventions [7–9]. Also, PMMA is non-resorbable, lacking the potential to remodel or integrate with existing bone, potentially complicating future procedures. Due to these limitations, there is interest in finding a resorbable implant material that immediately increases the strength of treated bone and maintains strength as it is resorbed and replaced by new bone [10]. The implant material should optimally have compressive strength and stiffness similar to normal bone, providing long-term functional benefit without negatively altering the long-term biomechanics of the fractured vertebral body being treated [10]. One such possible alternative implant material is an injectable in situ setting triphasic calcium-based implant, previously shown to strengthen cadaveric vertebral bodies [11].

A concern for all injectable materials used in vertebral augmentation is the possible adverse effect of extraosseous implant leakage which can cause severe complications including neurologic injury and pulmonary emboli [12–15]. The incidence of PMMA leakage is between 8–37% (18% average) during kyphoplasty and 34–80% (60% average) during vertebroplasty [12]. A particular concern for previously evaluated injectable resorbable calcium phosphate or calcium composite bone implant materials was stimulation of coagulation, as leakage with one formulation was reported to be associated with severe pulmonary vascular obstruction and formation of blood clots in the heart [16]. Studies demonstrated that other calcium composite implants lacked cohesion and disintegrated within the vasculature [17, 18], resulting in cardiovascular changes that were more severe when directly compared to PMMA [17].

The purpose of this study was to assess and compare the acute systemic effects of the triphasic calcium-based implant material, AGN1, to PMMA following direct injection into the femoral vein in a large animal sheep model.

Methods

Animals, preclinical model, and study design

Six skeletally mature, female, White Swiss Alpine sheep (mean age 4.6 years, range 3–7 years; mean weight 78.3 kg, range 66.5–91.5 kg) were enrolled in the study and randomly assigned to one of two groups ($n = 3$ sheep per group): PMMA or triphasic calcium implant material (AGN1). Each sheep underwent direct injection of 0.5 mL of implant material into the femoral vein to mimic cement volume leakage reported during PMMA vertebroplasty [19, 20]. Cardiopulmonary parameters and occurrence of sequela were monitored for 60 min after the injection procedure, as previously described (Fig. 1) [17, 18]. Afterward, the sheep were euthanized and underwent a systematic, complete postmortem inspection.

Prior to the start of the study, the sheep were acclimatized for at least 2 weeks and were in good health based on a complete physical assessment performed by a veterinarian and a complete blood cell count. To standardize the protocol, anesthesia monitoring was performed by the same anesthetist, catheter placement and implant injection were performed by the same surgeon, and the same support staff were present for each surgery. Experiments were carried out at an AAALAC International-approved facility and received ethical consent from the Veterinary Commission of the Canton of Grisons, Switzerland, in accordance with the Swiss laws of animal protection and welfare and were conducted under good laboratory practices (GLP). To minimize the risk of bias, the surgery staff and CT analysis personnel were blinded to the study group. The veterinary pathologist was also blinded to the study group during necropsy, histopathology and histomorphometry. The veterinary surgeon performed implant mixing and injection and thus was unblinded to the study groups.

Implant materials

PMMA bone cement was prepared (mixing and waiting phase) according to the manufacturer's instructions (BonOs, Osartis GmbH, Dieburg, Germany) and then transferred to 1 mL syringes. The triphasic calcium implant material (AGN1, AgNovos Healthcare LLC, Rockville, MD), composed of calcium sulfate, β-tricalcium phosphate, and brushite, was mixed for 30 s using the supplied mixer and then transferred to 1 mL syringes. PMMA or AGN1 were injected into the femoral veins via catheter following mixing and transfer at the earliest time possible (range 4 m:5 s to 4 m:20 s and 5 m:4 s to 5 m:20 s for PMMA and AGN1, respectively).

Preparation of animals

Sheep were sedated with xylazine 20 min before general anesthesia induction using intravenous midazolam and propofol, and endotracheally intubated for maintenance using sevoflurane in oxygen and air (targeted alveolar concentration of 1.5–2.0% sevoflurane in approximately 75% oxygen). Mechanical ventilation was instituted to maintain normocapnia with predefined settings (Table 1). Further modification to maintain all vital parameters in a physiological range was performed according to individual needs when deemed necessary by the anesthesiologist blinded to the study groups. Ventilator settings were not altered after implant injection.

Sheep were placed in dorsal recumbency, the inner thigh was aseptically prepared, and a 14G × 80-mm catheter was inserted into the femoral vein using the Seldinger technique under ultrasound guidance. Prior to injection,

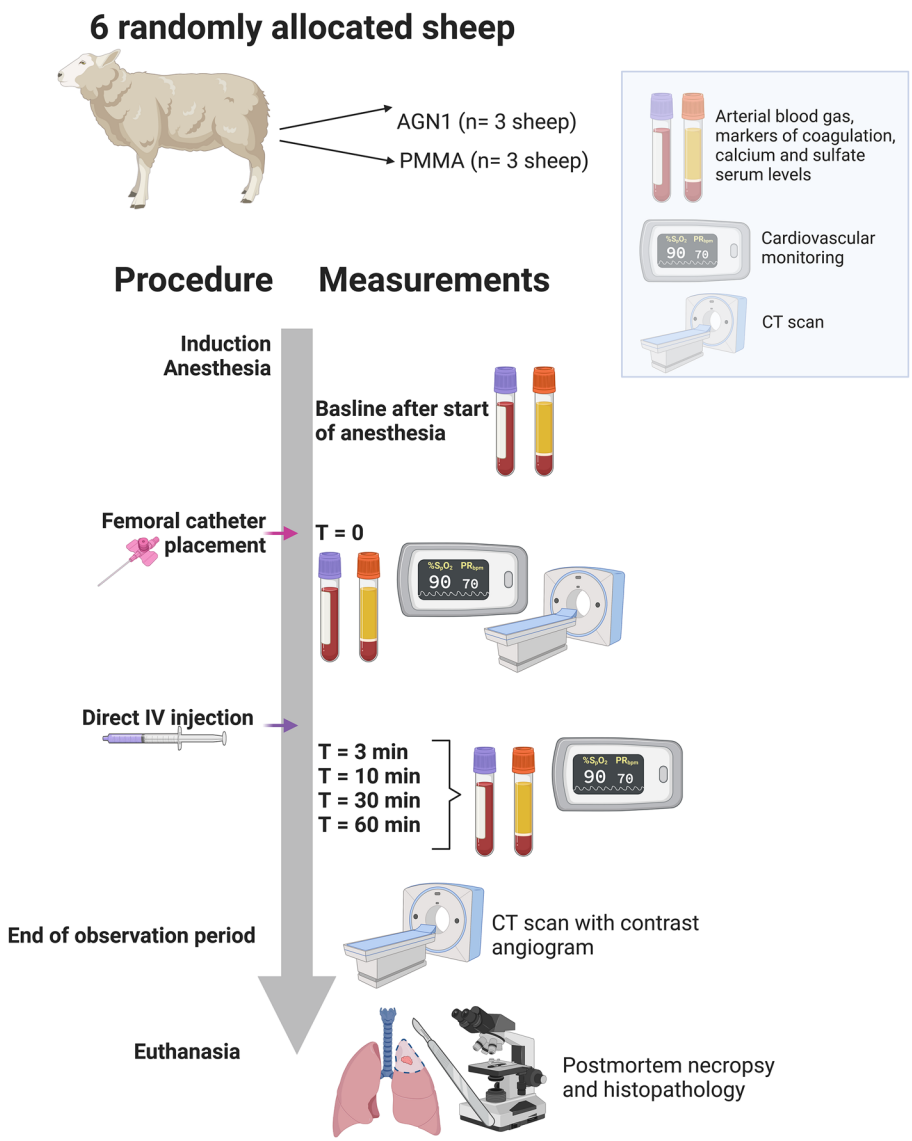

Fig. 1 Study design of in vivo sheep model mimicking severe clinical intravascular implant leakage. Schematics depicting the timeline of the interventions and main in vivo measurements at different time points (T) to assess and compare the systemic effects of a triphasic calcium-based implant material (AGN1) and polymethyl methacrylate (PMMA) injected directly into the femoral vein in a sheep model to mimic severe clinical intravascular implant leakage. Cardiovascular parameters, laboratory markers of coagulation, along with calcium and sulfate serum levels were monitored before and after implant injection. Afterward, the sheep were euthanized and underwent a systematic postmortem and histopathologic inspection

Table 1 Initial ventilator settings used for anesthesia

Ventilator parameters	Initial setting
Fraction of inspired oxygen	75%
Tidal volume	6–8 mL/kg
Respiratory rate	10–20 breaths per minute
Positive end expiratory pressure (PEEP)	5 cm H_2O
Inspiratory pressure (above PEEP)	15–20 cm H_2O
Inspiration/Expiration ratio	1:2

the catheter was flushed with saline. The catheter was then filled with the implant material, and immediately, thereafter, a single injection using a 1 mL syringe over a period of less than one minute resulted in systemic intravenous administration of 0.5 mL of implant material.

Cardiovascular monitoring

Systemic arterial blood pressure (mean (MABP), systolic, diastolic arterial blood pressure) was continuously recorded from a single lumen 20G catheter placed in the right auricular artery. Heart rate and blood oxygen saturation were also continuously recorded using an anesthesia monitor at 1 Hz (Datex Ohmeda S/5 Monitor; Anandic Medical Systems, Switzerland).

Blood sampling and analysis

Arterial and venous blood samples were taken prior to femoral catheter placement, prior to implant injection, and 3, 10, 30, and 60 min after implant injection (Fig. 1). A blood gas panel (pH, PCO_2, PO_2, tCO_2, HCO^3, sO_2, base excess, ionized calcium, Na, K, glucose, hematocrit, and hemoglobin)

was performed at each timepoint using arterial heparinized whole blood and a handheld analyzer (i-STAT® 1 Handheld Analyzer, Abbott, Princeton, NJ). Venous blood sampling was performed at each timepoint for total calcium, sulfate, D-dimer, and thrombin-antithrombin (TAT) complex analysis (see Appendix 1 for methodology details).

Computer tomography (CT) imaging and analysis

A clinical CT scan (Revolution EVO, GE Medical Systems (Schweiz) AG) examination of the thorax, abdomen and femoral catheter site was conducted prior to each injection procedure and after the 60-min observation (120 kV, 400 mAs, 0.625 mm slice thickness). A CT pulmonary angiography examination was also performed prior to euthanasia using a bolus tracking technique. Briefly, sequential axial slices were obtained at a set region of interest at the truncus pulmonalis during the contrast injection until a threshold enhancement (+60 HU) was met, triggering the diagnostic scan. Image reconstruction was done for the lungs with the standard kernel. Data were analyzed using Amira software (Amira 6.3, FEI SAS a part of Thermo Fisher Scientific).

The lungs were inspected slice by slice (2.5 mm slice thickness) in the native post-injection scan from cranial to caudal in the pulmonary window for hyperdense objects compared to the native pre-injection scan. The inferior vena cava and the femoral vein down to the injection site were also inspected slice by slice for hyperdense objects compared to the native pre-injection scan.

Euthanasia and tissue harvest

All animals were euthanized under general anesthesia by means of an intravenous overdose of barbiturate (Pentobarbital, Esconarkon) following final CT imaging. Comprehensive, systematic postmortem inspection with special attention to vital organs including brain, heart, and lungs was performed by a certified veterinary pathologist blinded to study groups. Lungs were fixed using instillation with 5% buffered formaldehyde solution then sampled (10 sites). Heart (3 sites), brain (7 sites), and all macroscopically changed tissue were sampled then immersed in fixative.

Histopathology and histomorphology analysis

Histopathological analysis and grading were performed by a certified veterinary pathologist blinded to study groups. Analyses focused on, but were not limited to, changes in vasculo-occlusive/thromboembolic events including thrombi, foreign material emboli, and hemorrhages. Changes present in tissue samples of the lungs, heart, brain, and representative macroscopically altered tissues were analyzed semi-quantitatively using a 6-point grading system (grade 0 to 5; grade 0: change absent, grade 5: massive severity).

A 1×1 cm^2 image of each lung slide (10 per sheep) was digitized using a $20\times$ objective and quantitatively analyzed for thromboembolic changes. Before starting to count, the image was divided into a total of 228 tiles ($12 \times 19\text{w} \times \text{h}$) using the digital reticle, resulting in individually numbered fields. The total number of thrombi, microthrombi, and capillary microthrombi were manually identified and automatically counted.

Statistics

A sample size of three per group only allowed for a qualitative analysis of the systemic effects of AGN1 leakage compared to PMMA. Descriptive statistics for measured parameters including mean, median, standard deviation, minimum, and maximum were reported, as appropriate, for each parameter.

Results

Cardiovascular monitoring and blood measurements

All sheep survived the 0.5 mL material injection and 60-min observation period. No difference was observed in cardiovascular parameters between the PMMA and AGN1 groups pre- and post-injection. After injection, changes in MABP, arterial oxygen content (SaO_2, PaO_2), and arterial carbon dioxide ($PaCO_2$) remained within physiological ranges in all sheep at all time points (Table 2). No difference was observed in calcium and sulfate between the PMMA and AGN1 groups pre- and post-injection (Table 3). Two sheep in the PMMA group had post-injection increases in thrombin-antithrombin (TAT), whereas no AGN1 animals had increases over pre-injection values (Fig. 2). D-dimer measurements were stable pre- and post-injection for both groups (D-dimer ≤ 0.6 ng/mL; data not shown).

CT analysis

CT imaging detected implant material in the lungs of one of three sheep in the PMMA group (Fig. 3A) and none of the AGN1 sheep (Fig. 3B). All six sheep had implant material in the abdominal vena cava and femoral vein (Fig. 3).

Pulmonary angiography indicated that there was no interruption of blood flow in the larger pulmonary vessels for either group.

Histopathology and histomorphology

Thrombotic changes at the lungs appeared less severe and less frequent for AGN1 compared to PMMA. The severity of thrombotic changes ranged from minimal (grade 1) to slight (grade 2) severity for the AGN1 group compared to minimal (grade 1) to massive severity (grade 5) for the PMMA group. The group medians were for thrombi: 0.0 versus 2.5; for microthrombi: 1.0 versus 3.5; and for capillary microthrombi: 0.0 versus 1.0 for AGN1 versus PMMA, respectively (Fig. 4). Thrombotic changes at the heart and brain were recorded at very low incidence and severity and not different between groups.

Quantification of thrombotic changes within the lungs demonstrated that the mean number of blood clots was fewer for AGN1 sections compared to PMMA sections (Fig. 5A−C; mean number per group: thrombi 0.7 versus 41.3; microthrombi 30.3 versus 191.0; and capillary microthrombi 30.3 versus 163.0, respectively). Neither PMMA nor AGN1 implant material were observed in any lung sections.

Additionally, a capillary obstruction complex was observed in the lungs of all three PMMA animals, but not in any of the AGN1 animals. This finding was characterized by increased capillary filling, increased number of neutrophils, and hemorrhage (Fig. 6). For the PMMA group, lung capillary obstruction complex severity ranged from grade 1 to grade 4, and the overall incidence across the 10 locations analyzed ranged from 20 to 90% for each animal.

Discussion

This is the first study to assess the acute and short-term physiologic and thromboembolic effects of intravascular injection of a resorbable, triphasic, calcium-based, osteoconductive implant material, AGN1, compared to PMMA. PMMA has a long history of use in vertebral augmentation despite frequent systemic leakage during the procedure and other complications [12]. In this study, the systemic

Table 2 Cardiovascular and blood gas data pre- and post-injection of PMMA and AGN1

		Pre-injection	3 min	10 min	30 min	60 min	Expected range [26, 27]
MABP (mmHg)	PMMA	64 (62–102)	65 (64–100)	64 (61–98)	75 (70–99)	84 (80–97)	70–110 mmHg
	AGN1	70 (65–100)	70 (67–100)	71 (63–100)	75 (66–103)	83 (82–105)	
Heart Rate (beats/min)	PMMA	87 (74–100)	NA	86 (77–98)	83 (83–95)	90 (79–92)	70–90 beats/min
	AGN1	90 (65–102)	NA	88 (64–103)	82 (61–102)	82 (61–99)	
SaO_2 (%)	PMMA	100 (100–100)	100 (100–100)	100 (100–100)	100 (100–100)	100 (100–100)	> 95%
	AGN1	100 (100–100)	100 (100–100)	100 (100–100)	100 (100–100)	100 (100–100)	
PaO_2 (mmHg)	PMMA	237 (99–258)	241 (105–276)	249 (99–249)	241 (102–263)	250 (105–284)	> 80 mmHg
	AGN1	213 (197–277)	231 (227–285)	217 (205–282)	245 (223–282)	237 (224–277)	
$PaCO_2$ (mmHg)	PMMA	44 (41–52)	47 (41–57)	46 (42–56)	49 (42–57)	47 (46–52)	35–45 mmHg; up to 80 mmHg during anesthesia
	AGN1	45 (35–56)	47 (46–55)	48 (47–55)	48 (47–57)	50 (47–57)	
pH	PMMA	7.46 (7.40–7.46)	7.46 (7.38–7.46)	7.46 (7.37–7.46)	7.44 (7.38–7.47)	7.44 (7.41–7.46)	7.35–7.45
	AGN1	7.47 (7.37–7.53)	7.48 (7.42–7.55)	7.48 (7.43–7.55)	7.47 (7.42–7.56)	7.48 (7.43–7.57)	
HCO_3^-(mmol/L)	PMMA	31.4 (28.8–31.9)	33.2 (28.7–33.3)	32.3 (29.8–33.0)	34.2 (28.2–35.1)	33.0 (31.4–33.8)	20–25 mmol/L
	AGN1	32.6 (28.9–32.6)	35.4 (34.6–41.1)	36.2 (34.6–41.7)	36.6 (35.5–42.5)	37.4 (36.5–42.7)	

Values are median and range ($n = 3$ per group)

Table 3 Ionized calcium, total calcium, and sulfate data pre- and post-injection of PMMA and AGN1

		Pre-injection	3 min	10 min	30 min	60 min	Expected range [26, 28–30]
Ionized Calcium (mmol/L)	PMMA	1.22 (1.17–1.22)	1.20 (1.16–1.22)	1.20 (1.12–1.21)	1.19 (1.17–1.20)	1.21 (1.18–1.21)	1.10—2.20 mmol/L
	AGN1	1.13 (1.05–1.19)	1.06 (1.05–1.16)	1.07 (0.99–1.16)	1.06 (1.01–1.18)	1.01 (1.00–1.14)	
Total Calcium (mmol/L)	PMMA	2.22 (2.09–2.24)	2.22 (2.09–2.24)	2.20 (2.08–2.23)	2.21 (2.08–2.23)	2.20 (2.06–2.25)	2.80—3.20 mmol/L
	AGN1	2.00 (1.94–2.40)	2.01 (1.97–2.39)	2.01 (1.96–2.39)	1.95 (1.93–2.38)	1.94 (1.89–2.33)	
Inorganic Sulfate (mg/dL)	PMMA	1.81 (1.80–2.01)	1.85 (1.83–2.00)	1.83 (1.77–1.91)	1.92 (1.73–2.01)	1.91 (1.71–1.92)	Not well characterized:11.9 mg/dL
	AGN1	1.70 (1.32–1.88)	1.77 (1.38–1.87)	1.74 (1.44–1.77)	1.72 (1.32–1.81)	1.78 (1.29–1.79)	

Values are median and range ($n=3$ per group)

effects of intravascular AGN1 appeared to be comparable to or less than that of intravascular PMMA. Similar cardiovascular and blood gas changes between both implant materials were observed. Although no blockage of the vasculature was observed via pulmonary angiography for either group, histopathological assessment revealed that the severity of thrombotic changes in the lungs was lower in the AGN1 group than in the PMMA group. No findings of capillary obstruction were observed in the AGN1 group, whereas the PMMA group had capillary obstruction to varying severity.

Direct implant material injection into the femoral vein of sheep was chosen to model severe clinical intravascular implant leakage that can occur during vertebral augmentation [12] or other orthopedic procedures [21] in which material injection has the potential for vascular leakage. The femoral vein drains to the inferior vena cava, where implant leakage is often detected clinically following vertebral augmentation [13] and where implant material was detected in all sheep included in this study. Implant material leakage into the inferior vena cava is significantly correlated with the development of pulmonary cement embolism [13]. An injection volume of 0.5 mL was chosen based on the volume of cement leakage reported during PMMA vertebroplasty averaging between 2.8% and 5.7% of the injected volume [19, 20]. An assumed injection volume of 8 mL and a worst-case assumption that all the material reaches the venous system translates to 0.46 mL of implant leakage. The 60-min follow-up to evaluate cardiopulmonary sequelae was based on the published literature in preclinical models as sufficient to evaluate those effects [17, 18].

Intravascular safety studies in large animals have been critical to the assessment of the potential clinical impact of leakage of alternative resorbable calcium-based implant materials. Bernard et al. demonstrated that a direct injection of a calcium phosphate implant resulted in a severe

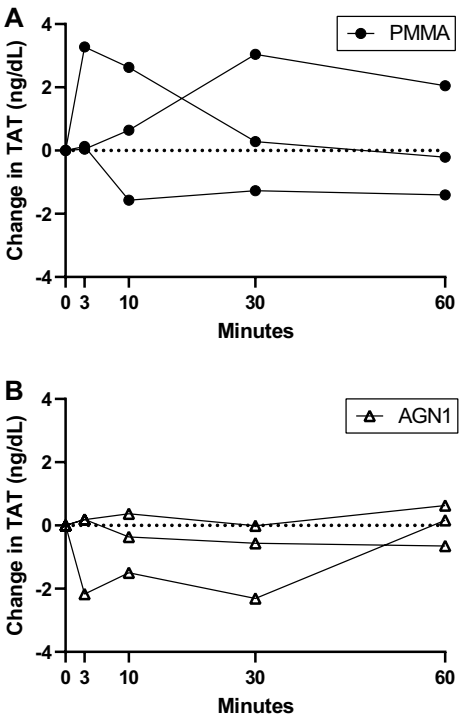

Fig. 2 Thrombin-antithrombin concentration. Change in thrombin-antithrombin (TAT) concentration (ng/dL) post-injection of PMMA ($n=3$) (**A**) and AGN1 ($n=3$) (**B**)

hypercoagulation reaction resulting in occlusion of the entire right ventricle and up to 86% mortality [16]. Krebs et al. found that a direct injection of a calcium phosphate implant resulted in increased pulmonary arterial pressure and decreased mean arterial blood pressure [17]. No similar changes were observed in this study following AGN1 injection. Qin et al. reported that a direct injection of a biphasic calcium sulfate/calcium phosphate resulted in smaller

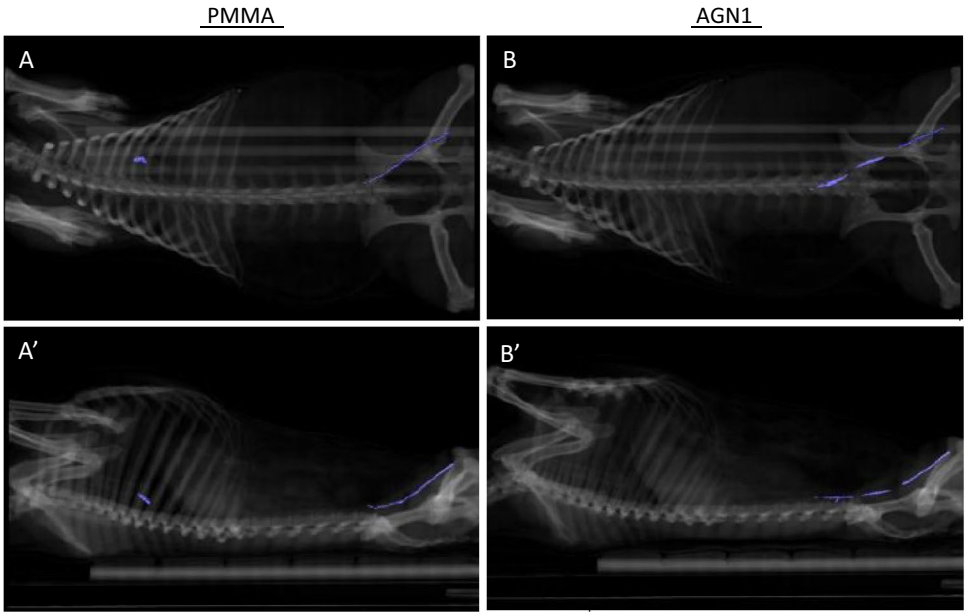

Fig. 3 CT Scan reconstruction. Digitally reconstructed post-injection CT images with the implant materials highlighted in color: PMMA (**A** and **A'**) and AGN1 (**B** and **B'**). Ventrodorsal (**A** and **B**) and latero-lateral (**A'** and **B'**) projections. PMMA cement was found in the vena cava and femoral vein (3 of 3 sheep) and lungs of 1 of 3 animals (**A**, **A'**). AGN1 implant material was found only in the vena cava and femoral vein (3 of 3 sheep; **B**, **B'**)

changes in pulmonary arterial pressure, mean arterial blood pressure, and blood gas when compared to PMMA [18].

The less frequent and less severe lung thrombotic changes in the AGN1 group were correlated with the reduced plasma levels of thrombin-antithrombin (TAT) which are known to be elevated during coagulation and in the procoagulant state [22]. TAT complex for all sheep remained below the reported physiological range (TAT ≤ 15 ng/mL) [23]; however, two PMMA sheep had TAT increases of 3 ng/mL after intravenous injection. Similar TAT increases following intravenous PMMA injection have been reported previously [18].

The lack of systemic activation of blood clotting by the triphasic AGN1 implant material used in this study has been reported for other, but not all, calcium phosphate formulations. Severe clot activation observed with one calcium phosphate formulation was hypothesized to be due to the implant material's surface morphology activating the coagulation pathway by providing a surface for clot formation combined with calcium released into the vasculature providing a cofactor for coagulation activation [16]. One suggestion for the relative lack of reactivity of the triphasic implant material in the present study is that the crystalline structure of the calcium sulfate, brushite and tricalcium phosphate in the implant material is less reactive and there is no increase in circulating levels of calcium after injection. An additional factor may be the lack of fragmentation or disintegration of the triphasic implant material following intravascular injection as reported with other injectable calcium phosphate materials [17, 18]. It has been hypothesized that cement disintegration could

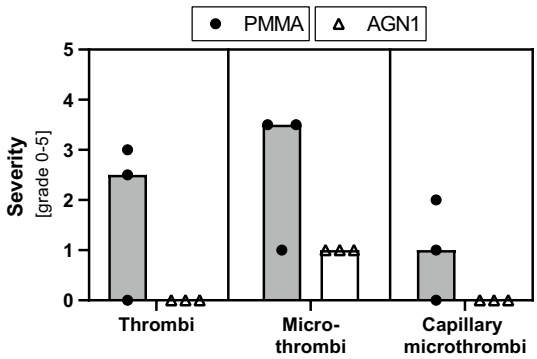

Fig. 4 Histopathologic semiquantitative assessment of severity of lung thrombotic changes assessed post-injection of PMMA and AGN1. Scale of 0 to 5 represents absent to massive severity. Bars represent median severity of the three animals; dots represent the median severity of ten different locations per animal

result in an increased number of emboli due to fragmentation and calcium ions released [17].

Strengths of this study are the clinically relevant sheep large animal model, the precise control of timing and implant material injection volumes directly into the venous circulation, the range of analyses performed, and the blinded nature of the study. The main limitation is the small sample size allowing only for qualitative comparisons. The short observation period and the differences between the animal model and actual clinical use are further limitations. Although inducing leakage in a vertebral body model would more closely mimic clinical usage, it would not allow control of the volume or location of the implant leakage into the vasculature system. Additionally,

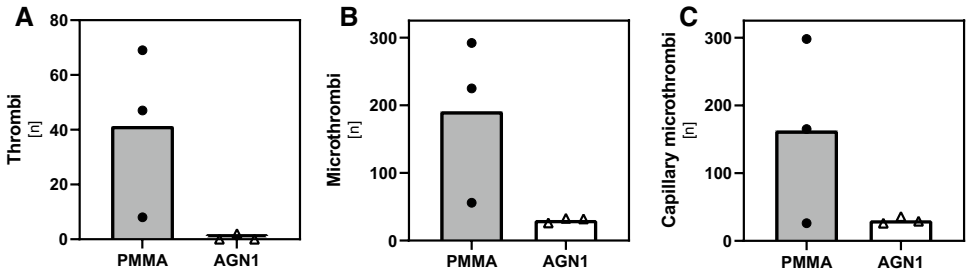

Fig. 5 Histomorphometric quantification of thrombotic changes within the lungs post-injection of PMMA and AGN1. Number of thrombi in large-sized vessels (**A**), in medium-sized vessels (**B**), and capillaries (**C**). Bars represent mean of the three animals; dots represent the sum of ten different locations per animal (each location 1 cm^2 in size)

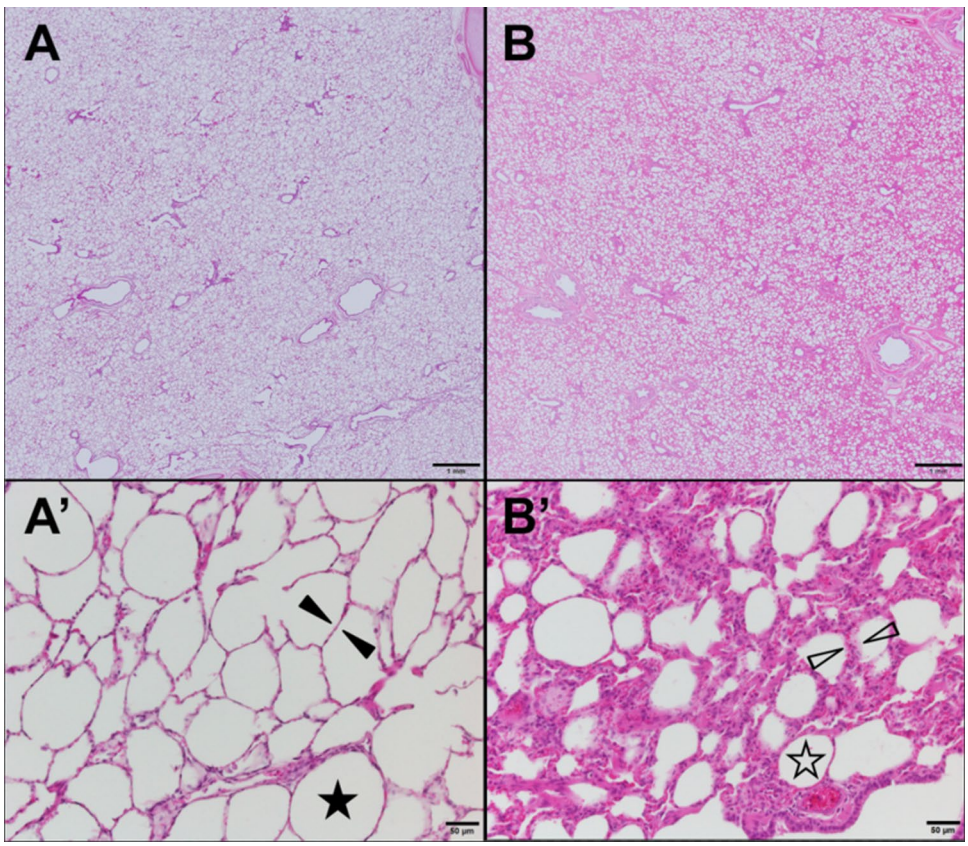

Fig. 6 Representative microphotography of pulmonary capillary obstruction complex observed post-injection at multiple locations within the lungs of all PMMA sheep. **A**, **A'**: unaffected location of a PMMA animal, **B**, **B'**: affected location of another PMMA animal, grade 4. **A** + **B** (lower magnification): Increased tissue density (**B**), compared to (**A**) an unaffected location. **A'** + **B'** (higher magnification): Note the thickening of the alveolar blood barrier (open arrows), and the decreased alveolar space (open asterisk) caused by increased capillary filling combined with neutrophils, hemorrhage (Hematoxylin and eosin-stained sections; scale bars 1 mm (**A**, **B**) and 50 µm (**A'**, **B'**)

inducing leakage into a vertebral body as the result of implant injection would produce fat emboli, potentially masking the effect of implant material leakage [24, 25].

Conclusion

This study demonstrated that the acute systemic and thromboembolic effects of a direct injection of a triphasic calcium-based implant material into the femoral vein appear to be comparable to or less than the effects of an injection of PMMA bone cement. Specifically, the severity and incidence of pulmonary histological changes may be lower for AGN1 compared to PMMA; however, a larger study would be required to determine whether these data are statistically significant. These preliminary safety data are supportive of further clinical evaluation of the implant material for vertebral augmentation.

Supplementary Information The online version contains supplementary material available at https://doi.org/10.1007/s00586-022-07303-x.

Author contributions All authors contributed to the study conception and design. Study preparation, data collection and analysis were performed by CC, AR, DK, DG, and UM. The first draft of the manuscript was written by CC and JDS. The manuscript was critically revised by SZ, LMB, RSH, and CEA. All authors read and approved the final manuscript.

Funding This work was funded by AgNovos Healthcare.

Declarations

Conflict of interest John D. Stroncek and Ronald S. Hill are employed by AgNovos Healthcare. Lorin Benneker and Christoph Albers have received honoraria from AgNovos Healthcare. The remaining authors have no conflicts of interest.

References

1. McCarthy J, Davis A (2016) Diagnosis and management of vertebral compression fractures. Am Fam Physician 94:44–50
2. Edidin AA, Ong KL, Lau E, Kurtz SM (2011) Mortality risk for operated and nonoperated vertebral fracture patients in the medicare population. J Bone Miner Res 26:1617–1626. https://doi.org/10.1002/jbmr.353
3. Lange A, Kasperk C, Alvares L et al (2014) Survival and cost comparison of kyphoplasty and percutaneous vertebroplasty using german claims data. Spine 39:318–326. https://doi.org/10.1097/BRS.0000000000000135
4. Tsoumakidou G, Too CW, Koch G et al (2017) CIRSE guidelines on percutaneous vertebral augmentation. Cardiovasc Intervent Radiol 40:331–342. https://doi.org/10.1007/s00270-017-1574-8
5. Hirsch JA, Beall DP, Chambers MR et al (2018) Management of vertebral fragility fractures: a clinical care pathway developed by a multispecialty panel using the RAND/UCLA appropriateness method. Spine J 18:2152–2161. https://doi.org/10.1016/j.spinee.2018.07.025
6. Hirsch JA, Chandra RV, Carter NS et al (2019) Number needed to treat with vertebral augmentation to save a life. AJNR Am J Neuroradiol. https://doi.org/10.3174/ajnr.A6367
7. Lewis G (1997) Properties of acrylic bone cement: state of the art review. J Biomed Mater Res 38:155–182. https://doi.org/10.1002/(SICI)1097-4636(199722)38:2%3c155::AID-JBM10%3e3.0.CO;2-C
8. Nagaraja S, Awada HK, Dreher ML et al (2013) Vertebroplasty increases compression of adjacent IVDs and vertebrae in osteoporotic spines. Spine J 13:1872–1880. https://doi.org/10.1016/j.spinee.2013.06.007
9. Cho A-R, Cho S-B, Lee J-H, Kim K-H (2015) Effect of augmentation material stiffness on adjacent vertebrae after osteoporotic vertebroplasty using finite element analysis with different loading methods. Pain Physician 18:E1101–E1110
10. Lewis G (2006) Injectable bone cements for use in vertebroplasty and kyphoplasty: state-of-the-art review. J Biomed Mater Res Part B Appl Biomater 76:456–468. https://doi.org/10.1002/jbm.b.30398
11. Trost M, Schmoelz W, Wimmer D et al (2020) Local osteoenhancement of osteoporotic vertebra with a triphasic bone implant material increases strength—a biomechanical study. Arch Orthop Trauma Surg 140:1395–1401. https://doi.org/10.1007/s00402-020-03382-x
12. Zhan Y, Jiang J, Liao H et al (2017) Risk factors for cement leakage after vertebroplasty or kyphoplasty: a meta-analysis of published evidence. World Neurosurg 101:633–642. https://doi.org/10.1016/j.wneu.2017.01.124
13. Kim YJ, Lee JW, Park KW et al (2009) Pulmonary cement embolism after percutaneous vertebroplasty in osteoporotic vertebral compression fractures: incidence, characteristics, and risk factors. Radiology 251:250–259. https://doi.org/10.1148/radiol.2511080854
14. Hassani SF, Cormier E, Shotar E et al (2018) Intracardiac cement embolism during percutaneous vertebroplasty: incidence, risk factors and clinical management. Eur Radiol. https://doi.org/10.1007/s00330-018-5647-0
15. Weininger G, Elefteriades JA (2021) Intracardiac cement embolism. N Engl J Med 385:e49. https://doi.org/10.1056/NEJMicm2032931
16. Bernards C, Chapman J, Mirza S (2004) Lethality of embolized norian bone cement varies with the time between mixing and embolization. Proc 50th Annu Meet Orthop Res Soc 254
17. Krebs J, Aebli N, Goss BG et al (2007) Cardiovascular changes after pulmonary embolism from injecting calcium phosphate cement. J Biomed Mater Res - Part B Appl Biomater 82:526–532. https://doi.org/10.1002/jbm.b.30758
18. Qin Y, Ye J, Wang P et al (2016) Evaluation of the biphasic calcium composite (BCC), a novel bone cement, in a minipig model of pulmonary embolism. J Biomater Sci Polym Ed 27:317–326. https://doi.org/10.1080/09205063.2015.1128240
19. Jin YJ, Yoon SH, Park K-W et al (2011) The volumetric analysis of cement in vertebroplasty. Spine 36:E761–E772. https://doi.org/10.1097/BRS.0b013e3181fc914e
20. Bae H, Hatten HP, Linovitz R et al (2012) A prospective randomized FDA-IDE trial comparing cortoss with PMMA for vertebroplasty: a comparative effectiveness research study with 24-month follow-up. Spine 37:544–550. https://doi.org/10.1097/BRS.0b013e31822ba50b
21. Hines CB (2018) Understanding bone cement implantation syndrome. AANA J 86:433–441
22. Vervloet M, Thijs L, Hack C (1998) Derangements of coagulation and fibrinolysis in critically III patients with sepsis and septic shock. Semin Thromb Hemost 24:33–44. https://doi.org/10.1055/s-2007-995821
23. Lavaud S, Canivet E, Wuillai A et al (2003) Optimal anticoagulation strategy in haemodialysis with heparin-coated polyacrylonitrile membrane. Nephrol Dial Transpl 18:2097–2104. https://doi.org/10.1093/ndt/gfg272
24. Aebli N, Krebs J, Davis G et al (2002) Fat embolism and acute hypotension during vertebroplasty: an experimental study in sheep. Spine 27:460–466
25. Krebs J, Ferguson SJ, Hoerstrup SP et al (2008) Influence of bone marrow fat embolism on coagulation activation in an ovine. J Bone Joint Surg 90:349–356. https://doi.org/10.2106/JBJS.G.00058
26. Grimm KA, Lamont LA, Tranquilli WJ et al (2015) Veterinary anesthesia and analgesia, the fith edition of Lumb and Jones. Wiley, Hoboken

27. Kaneko JJ, Harvey JW, Bruss ML (2008) Clinical biochemistry of domestic animals. Academic Press
28. Duncan J, Prasse K (1986) Vertinary laboratory medicine, 2nd edn. Iowa State University Press
29. Smith B, Van Metre D, Pusterla N (2019) Large animal internal medicine, 6th edn. Mosby, United States
30. Krugsheld KR, Scholtens E, Mulder GJ (1980) Serum concentration of inorganic sulfate in mammals: species differences and circadian rhythm. Comp Biochem Physiol Part A Physiol 67:683–686. https://doi.org/10.1016/0300-9629(80)90261-3